Latest developments in molecular tracers for fluorescence image-guided cancer surgery

Sophie Hernot, Labrinus van Manen, Pieterjan Debie, Jan Sven David Mieog, Alexander Lucas Vahrmeijer

Real-time intraoperative guidance is essential during oncological surgery for complete and safe tumour resection. Fluorescence imaging in the near-infrared spectrum has shown potential for guiding surgeons during complex interventions. Recently, there has been a shift towards the use of fluorescence contrast agents for molecular imaging. The first targeted fluorescent agents, of which most consist of approved therapeutic antibodies conjugated to a fluorescent dye, have been evaluated in several early-phase clinical trials. Moreover, advances in protein engineering and drug design have led to the development of a variety of tracers suitable for molecular fluorescence image-guided surgery. In this Review, we discuss preclinical and clinical evidence, ongoing clinical trials, and the latest developments in the field of molecular near-infrared tracers for fluorescence-guided cancer surgery.

Lancet Oncol 2019; 20: e354–67

Laboratory for In-vivo Cellular and Molecular Imaging, Vrije Universiteit Brussel, Brussels, Belgium (Prof S Hernot PhD, P Debie MSc)**; and Department of Surgery, Leiden University Medical Center, Leiden, Netherlands** (L van Manen BSc, J S D Mieog MD, A L Vahrmeijer MD)

Correspondence to:
Prof Sophie Hernot, Laboratory for In-vivo Cellular and Molecular Imaging Vrije Universiteit Brussel, Laarbeeklaan 103, 1090 Brussels, Belgium
sophie.hernot@vub.be

Introduction

Surgery is pivotal in the treatment of solid cancers. Unfortunately, tumour-positive resection margins occur in 8–70% of cases depending on the cancer type.[1–4] Because complete removal of tumour tissue is mandatory for prolonged survival and to preserve as much healthy tissue as possible, intraoperative guidance is essential to surgeons. Besides using visual (based on white light reflectance) and tactile feedback, surgeons can use ultrasound imaging as an additional tool for intraoperative guidance in selected cases, but this tool alone is often insufficient.[5] Other imaging techniques, such as x-ray, CT, or MRI are mainly used for surgical planning or interim assessment because they do not provide real-time intraoperative guidance. Recently, surgeons have started to use fluorescent light for surgical navigation.

Fluorescence imaging uses a specialised camera to capture light emitted by a fluorescent contrast agent after excitation with an appropriate light source. All imaging equipment can be integrated into a compact open-field device or within laparoscopic or robotic instruments for contact-free and real-time interrogation (figure 1). The fluorescent contrast agent is administered to visualise the organ or tissue of interest with sufficient sensitivity and contrast. For medical applications, fluorescent agents that emit at wavelengths in the near-infrared region, between 650 and 800 nm, are more advantageous than those emitting visual light. Near infrared light can penetrate deeper into tissue (up to several mm) with less scattering than visual light and there is less autofluorescence.[6]

Indocyanine green and methylene blue are the only available near-infrared fluorophores that are approved by the US Food and Drug Administration. Indocyanine green is mainly used for the evaluation of blood flow, sentinel lymph node mapping, and liver tumour imaging.[7] Methylene blue has been evaluated for ureter, thyroid nodule, and neuroendocrine tumour visualisation; however, it is currently not used in regular surgical care due to its non-specificity and limited quantum yield. Besides indocyanine green and methylene blue, 5-aminolevulinic acid and its derivate 5-aminolevulinic acid hexyl ester, are two non-fluorescent prodrugs that are both clinically approved for imaging of malignant gliomas and bladder cancer, respectively. These prodrugs elicit the synthesis of fluorescent protoporphyrin IX (maximal emission peak around 634 nm, thus just outside the near-infrared region), which accumulates in malignant tumour tissue. Two randomised controlled phase 3 trials[8,9] have shown improved resection margins and increased progression-free survival for patients with malignant gliomas and bladder cancer. However, drawbacks of fluorescence imaging with 5-aminolevulinic acid include inhomogeneous signals that are dependent on the tumour grade, absence of penetration depth, and photobleaching.[10] Over recent years there has been a shift from structural and functional fluorescence imaging to molecular fluorescence imaging using more specific fluorescent agents (figure 2). Molecular fluorescence imaging could be used for many applications relevant to oncological surgery such as the detection of occult tumour lesions, assessment of tumour margins and locoregional invasion, and emphasis on vital structures (figure 1).[11] In this Review, we focus on the clinical evidence in molecular near-infrared fluorescence-guided cancer surgery and latest developments regarding molecular probes in the field.

Targeted fluorescent agents under evaluation in clinical trials

The specific accumulation of a fluorescent contrast agent in a tissue of interest requires stable conjugation of a fluorophore to a targeting molecule. The targeted cells, most often cancer cells, will thus literally light up, whereas the background is expected to be significantly less fluorescent once the unbound tracer has cleared. Several tumour-specific ligands, recognising diverse molecular biomarkers, have been evaluated for molecular fluorescence imaging applications in the clinic. An overview of published and ongoing clinical trials is provided in table 1.

In 2011, van Dam and colleagues[12] did the first targeted fluorescence molecular imaging trial by using the contrast agent EC-17, which consists of folic acid

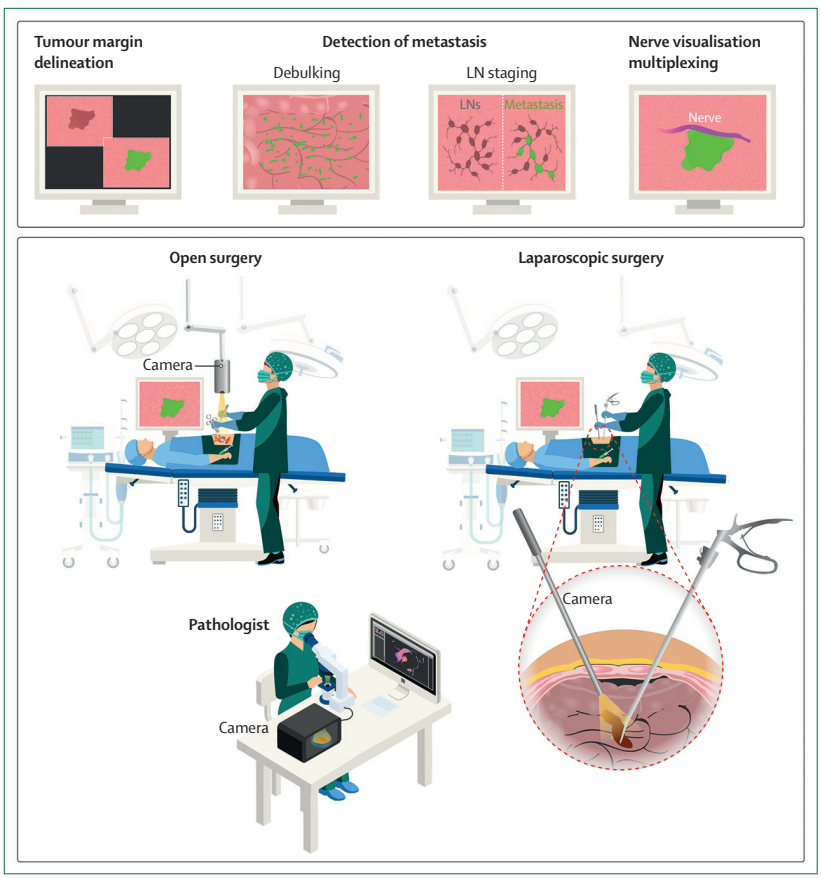

Figure 1: **Principle of intraoperative molecular near-infrared (NIR) fluorescence imaging**
(Top) Schematic illustration of potential applications of molecular targeted NIR fluorescence imaging. (Bottom) Implementation of fluorescence guidance during open and laparoscopic surgery. After intravenous injection of the tracer (1 h up to several days before surgery depending on the tracer), the tumour or other tissues of interest can be visualised with a specialised NIR camera, thereby guiding the surgeon in real-time during resection. Immediately after resection, the specimen(s) can be imaged on a back table (a table in the operating room equipped to analyse tissue samples) with a fluorescence camera and microscope. The pathologist can thus rapidly check resection margins on the presence of fluorescence and provide rapid feedback to the surgeon.

conjugated with fluorescein isothiocyanate (emission 520 nm), in patients with ovarian cancer during cytoreductive surgery. In three patients, folate receptor-α expressing malignant tumour deposits could be clearly identified intraoperatively and distinguished from benign structures. Similar results were found for lung, breast, and renal tumours.[13–16] However, the limited penetration of light and relatively high autofluorescence signal from collagen-rich tissues in this wavelength range turned out to be suboptimal. Consequently, the analogous fluorescent tracer OTL-38, also targeting folate receptor, but emitting at 796 nm, was developed and tested in several cancer types, including ovarian, lung, renal, and endometrial tumours, as well as meningioma.[17–26] Hoogstins and colleagues[17] showed in 12 patients with ovarian cancer that surgeons were able to detect 29% additional malignant lesions during debulking surgery, which were not detected using visual inspection. Other pilot studies showed that pulmonary adenocarcinomas could be detected with a sensitivity of up to 100%,[23] and squamous cell carcinomas with up to 70%.[21] Furthermore, in-situ fluorescence imaging even appeared to be superior to ^{18}F-FDG-PET for the detection of malignant pulmonary nodules.[19] A larger multicentre international phase 2 trial (NCT02872701) determining the clinical efficacy in terms of detection of additional tumour-positive nodules, synchronous lesions, and tumour-positive margins during lung surgery in 110 patients has been completed, but results are not published yet. In another trial,[26] endometrial cancer, including omental and lymph node metastases, could also be detected using OTL-38 in four patients. Nevertheless, a high rate of false-positive signals (34%) was recorded, which was caused by non-specific targeting of OTL-38 to folate receptor-β in non-metastatic lymph nodes.

Alternatively, tozuleristide is a naturally occurring knotted peptide conjugated to indocyanine green. This tracer has known affinities for matrix metalloproteinase-2 and annexin A2, which are expressed in a variety of solid tumours. Dintzis and colleagues[43] showed that tozuleristide, when administered between 1 to 26 h before surgery, enabled detection of tumour tissue in freshly resected pathology specimens of 23 patients with breast cancer. Phase 1 studies (NCT02234297 and NCT02462629) in paediatric and adult patients with CNS tumours have been completed and a randomised phase 2/3 trial (NCT03579602) has started recruiting patients.

With the introduction of the commercially available near-infrared fluorophore IRDye800CW, existing therapeutic monoclonal antibodies could quite easily be repurposed after fluorescence labelling. For example, bevacizumab-IRDye800CW has been used in various clinical feasibility trials targeting tumours that overexpress vascular endothelial growth factor. Harlaar and colleagues[27] studied seven patients with peritoneal carcinomatosis of colorectal origin undergoing cytoreductive surgery and showed that fluorescence imaging with bevacizumab-IRDye800CW enabled in-situ detection of additional malignant lesions, while

Figure 2: **Molecular fluorescent contrast agents and targeting moieties used for intraoperative imaging during cancer surgery**
(A) Schematic representation of the mode of action of the different types of fluorescent contrast agents. Non-targeted fluorescent contrast agents such as indocyanine green passively accumulate in tumour tissue via the enhanced permeability and retention effect. Targeted fluorescent contrast agents, consisting of a fluorescent dye conjugated to a targeting moiety, actively accumulate in tumour tissue by recognition of a specific biomarker expressed by tumour cells or tumour-associated stromal cells. Imaging is performed once unbound tracers have been cleared sufficiently. Activatable fluorescent contrast agents remain optically silent until fluorescent dyes are released by enzymatic digestion of their backbone. (B) Schematic representation of the different classes and subclasses of targeting moieties used for the design of targeted fluorescent contrast agents: antibodies, antibody fragments, protein scaffolds, peptides and small molecules. Representative space-filling images of an antibody (1IGT), Fab-fragment (6B9Z), diabody (1MOE), scFv (1P4I), nanobody (5MY6), centyrin (5L2H), affibody (2KZJ) and knottin (2N8B) were obtained from the RCSB protein bank and prepared using PyMOL. The space-filling minibody model is an interpretation created using PyMOL; antigen-binding regions are highlighted in orange.

fluorescence uptake was absent in clinically suspicious but benign lesions. Contrarily, for breast cancer surgery, a dose of 4·5 mg of bevacizumab-IRDye800CW, which falls under the microdosing regimen, was too low to enable in-situ margin assessment.[28] Tumour-positive margins could nevertheless be detected ex-vivo after bread-loaf slicing (a common method of processing surgical specimens for histopathology) on the back table.[28] These results show the relevance of developing fluorescence-guided intraoperative pathology that could provide fast

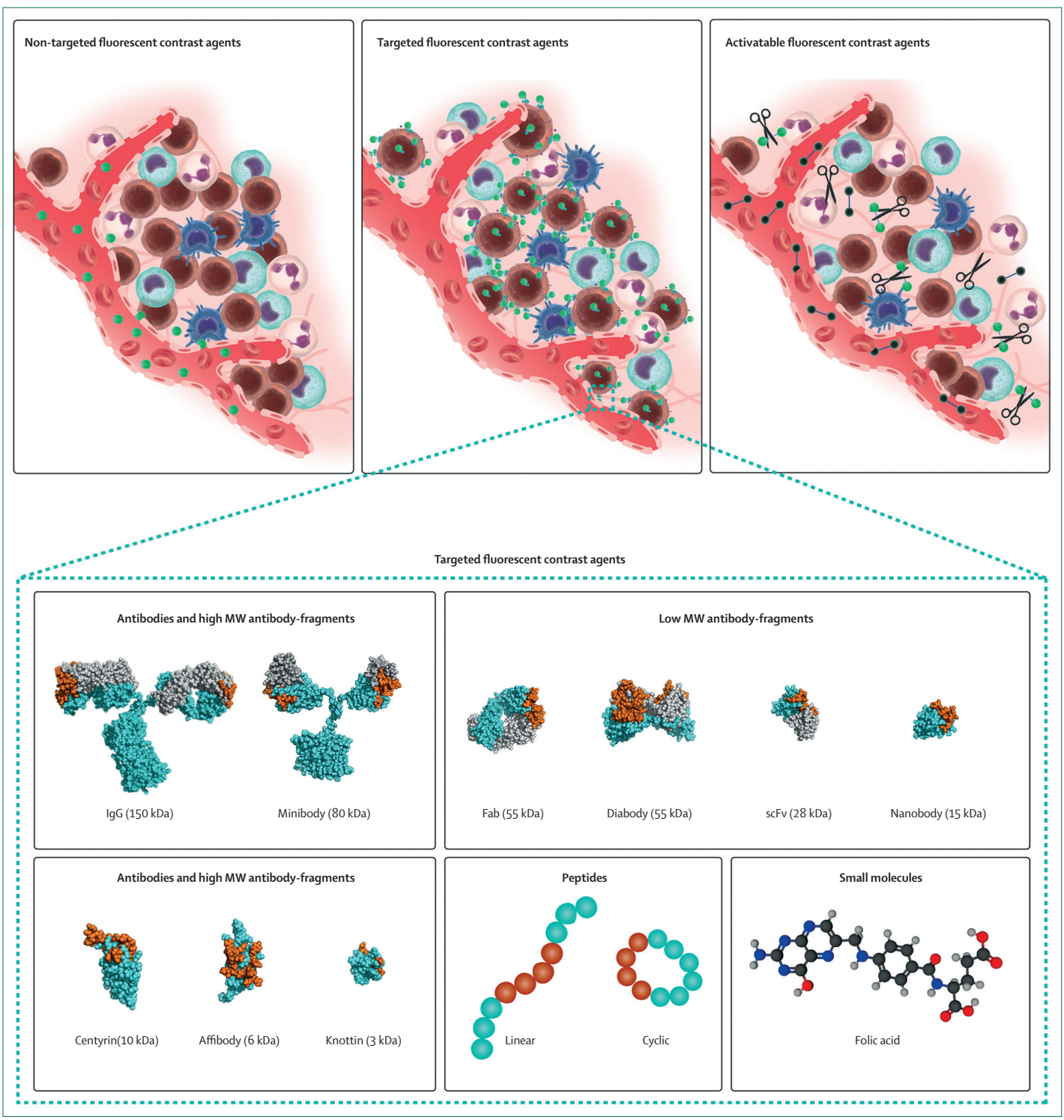

	Target	Target tissue	Study type	Study population (n)	Incorporation	Interval between injection and surgery	Others
EC17[12]	Folate receptor	Ovarian cancer	Phase 1	10	Open (cytoreductive) surgery	2–8 h	..
EC17[13]	Folate receptor	Lung cancer	Phase 1	30	Open surgery or VATS	4 h	..
EC17[14]	Folate receptor	Lung cancer	Phase 1	50	Open surgery	4 h	..
EC17[15]	Folate receptor	Breast and ovarian cancer	Phase 1	15:12 ovarian; 3 breast cancer	Open surgery	2–3 h	..
EC17[16]	Folate receptor	Renal cell carcinoma	Case report	4	Open surgery	4 h	..
EC17 (NCT01778933)	Folate receptor	Renal cell carcinoma	Phase 1	10	Open or laparoscopic surgery	2–4 h	..
OTL38[17]	Folate receptor	Ovarian cancer	Phase 1a/1b	42	Open (debulking) surgery	2–3 h	Phase 1a: 30 healthy volunteers; phase 1b: 12 patients
OTL38 (NCT03180307)	Folate receptor	Ovarian cancer	Phase 3	147	Open (debulking) surgery	..	..
OTL38[18]	Folate receptor	Renal cancer	Case report	3	Robotic surgery	2 h	..
OTL38 (NCT02645409)	Folate receptor	Renal cancer	Phase 2	20	..	2 h	..
OTL38[19]	Folate receptor	Pulmonary adenocarcinoma	Phase 1	50	VATS, robotic surgery	3–6 h	Combined with PET-CT
OTL38[20]	Folate receptor	Pulmonary adenocarcinoma	Case report	1	VATS	3–6 h	..
OTL38[21]	Folate receptor	Pulmonary squamous cell carcinoma	Phase 1	12	VATS	3–6 h	..
OTL38[22]	Folate receptor	Pulmonary adenocarcinoma	Phase 1	20	VATS	3–6 h	..
OTL38[23]	Folate receptor	Pulmonary adenocarcinoma	Phase 1	10	VATS	3–6 h	..
OTL38[24]	Folate receptor	Pulmonary ground glass opacities	Phase 1	20	VATS	3–6 h	..
OTL38 (NCT02872701)	Folate receptor	Pulmonary adenocarcinoma	Phase 2 (multicenter)	110	VATS	2–3 h	..
OTL38[25]	Folate receptor	Meningioma	Case report	1	Open surgery	..	..
OTL38[26]	Folate receptor	Endometrium	Phase 1	4	Open surgery	2–3 h	..
Bevacizumab-IRDye800CW[27]	VEGF	Colorectal peritoneal metastases	Phase 1	7	Open surgery	2 days	..
Bevacizumab-IRDye800CW[28]	VEGF	Breast cancer	Phase 1	20	Open surgery	3 days	..
Bevacizumab-IRDye800CW (NCT02975219)	VEGF	Endometriosis	Phase 1	10	..	3 days	..
Bevacizumab-IRDye800CW (NCT02743975)	VEGF	Pancreatic cancer	Phase 1/2	26	Open surgery	3 days	..
Bevacizumab-IRDye800CW (NCT03620292)	VEGF	Perihilar cholangiocarcinoma	Phase 1/2	12	Open surgery	3 days	Including ex vivo endoscopic fluorescence imaging of resected specimen
Cetuximab-IRDye800CW[29]	EGFR	Head and neck cancer	Phase 1	9	Open surgery	3–4 days	Dose-escalation study; fluorescence imaging was only conducted ex-vivo on resected specimens
Cetuximab-IRDye800CW[30]	EGFR	Head and neck cancer	Phase 1	12	Open surgery	3–4 days	Dose-escalation study
Cetuximab-IRDye800CW[31]	EGFR	Head and neck cancer	Phase 1	12	Open surgery	3–7 days	Dose-escalation study
Cetuximab-IRDye800CW[32]	EGFR	Head and neck cancer	Phase 1a	12	Open surgery	1–5 days	Dose-escalation study evaluating both cetuximab-IRDye800CW and panitumumab-IRDye800CW

(Table 1 continues on next page)

	Target	Target tissue	Study type	Study population (n)	Incorporation	Interval between injection and surgery	Others
(Continued from previous page)							
Cetuximab-IRDye800CW (NCT03134846)	EGFR	Head and neck cancer	Phase 1/2	79	Open surgery	4 days	Dose-escalation in nine patients; expansion cohort in 70 patients
Cetuximab-IRDye800CW[33]	EGFR	Pancreatic cancer	Phase 1	7	Open and laparoscopic surgery	2–5 days	Photoacoustic imaging was also performed
Cetuximab-IRDye800CW[34]	EGFR	Pancreatic cancer	Phase 1	7	Open surgery	2–5 days	Dose-escalation study
Cetuximab-IRDye800CW[35]	EGFR	Glioblastoma	Case report	3	Open surgery	2 days	..
Panitumumab-IRDye800CW[32]	EGFR	Head and neck cancer	Phase 1a	15	Open surgery	1–5 days	Dose-escalation study evaluating both cetuximab-IRDye800CW and panitumumab-IRDye800CW
Panitumumab-IRDye800CW[36]	EGFR	Head and neck cancer	Phase 1	21	Open surgery	1–5 days	..
Panitumumab-IRDye800CW[37]	EGFR	Oral squamous cell carcinoma	Phase 1	8	Open surgery	1–4 days	..
Panitumumab-IRDye800CW[38]	EGFR	Head and neck cancer	Phase 1	14	Open surgery	1–5 days	..
Panitumumab-IRDye800CW (NCT03384238)	EGFR	Pancreatic cancer	Phase 1/2	24	Open or laparoscopic surgery	2–5 days	..
Panitumumab-IRDye800CW (NCT03510208)	EGFR	Malignant glioma	Phase 1/2	22	Open surgery	1–5 days	..
Panitumumab-IRDye800CW (NCT03582124)	EGFR	Lung carcinoma	Phase 1/2	30	..	1–5 days	..
Panitumumab-IRDye800CW (NCT03405142)	EGFR	Head and neck cancer	Phase 2	20	Open surgery	2–5 days	Focussing on lymph node detection by comparing near infrared fluorescence with lymphoscintigraphy and SPECT/CT after injection of ^{99m}Tc-labelled tilmanocept
SGM-101[39]	CEA	Pancreatic cancer	Phase 1	12	Open surgery	2–4 days	..
SGM-101[40]	CEA	Colorectal cancer	Phase 1/2	26	Open and laparoscopic surgery	2–4 days	..
SGM-101 (NCT03659448)	CEA	Colorectal cancer	Phase 3 (randomised controlled trial)	300	Open and laparoscopic surgery	2–4 days	..
^{111}In-DOTA-Labetuzumab-IRDye800CW (NCT03699332)	CEA	Colorectal peritoneal metastases	Phase 1/2	29	Open surgery	6–7 days	Dual modality imaging
^{111}In-DOTA-Girentuximab-IRDye800CW[41]	CAIX	Renal cancer	Phase 1	15	Open surgery	7 days	Dual modality imaging
^{68}Ga-NOTA-IRDye800CW-BBN[42]	GRPR	Glioblastoma	Phase 1	14	Open surgery	2 h	Dual modality imaging
Tozuleristide (BLZ-100)[43]	Cell-surface chlorotoxin binding proteins	Breast cancer	Phase 1	23	Open surgery	1–26 h	Fluorescence imaging was only conducted ex-vivo on resected specimens
Tozuleristide (BLZ-100) (NCT02234297)	Cell-surface chlorotoxin binding proteins	Glioma	Phase 1	17	Open surgery	2 h	..
Tozuleristide (BLZ-100) (NCT02462629)	Cell-surface chlorotoxin binding proteins	CNS tumours	Phase 1	32	Open surgery	1 h	Dose escalation and expansion cohort in paediatric subjects

(Table 1 continues on next page)

	Target	Target tissue	Study type	Study population (n)	Incorporation	Interval between injection and surgery	Others
(Continued from previous page)							
Tozuleristide (BLZ-100) (NCT03579602)	Cell-surface chlorotoxin binding proteins	CNS tumours	Phase 2/3 (randomised controlled trial)	114	Open surgery	1–36 h	Subjects will be randomised 1:10 to 1 of 2 study arms; study arm 1: no BLZ-100 injection, although imaging will be performed; study arm 2: BLZ-100 injection and imaging will be done
VB5–845D-800CW (NL7363)	EpCam	Oesophageal/gastric or rectosigmoid cancer	Phase 1	34	Laparoscopic surgery	Optimal injection time will be based on the results of part 1a	Part 1a: dose escalation in human volunteers (n=16); part 1b: dose optimisation in patients (n=18)
ABY029 (NCT02901925)	EGFR	Recurrent glioma	Phase 1a	12	Open surgery	1–3 h	..
ABY029 (NCT03154411)	EGFR	Sarcoma	Phase 1a	18	Open surgery	1–3 h	..
ABY029 (NCT03282461)	EGFR	Head and neck cancer	Phase 1a	12	Open surgery	1–3 h	..
IR800 IAb2M (ISRCTN10046036)	PSMA	Prostate cancer	Phase 1	120	Robot-assisted laparoscopic surgery	1–2 days	Part one: dose escalation in 20 patients; part two: randomised allocation of IR800 IAb2M in 100 patients
cRGD-ZW800–1 (NL7724)	Integrins (associated with tumour angiogenesis)	Colorectal cancer	Phase 2	12	Laparoscopic surgery	<24 h	Ureter could also be visualised simultaneously, due to characteristics of ZW800–1
HS-196 (NCT03333031)	HSP-90 inhibitor	Breast cancer	Phase 1	120	Open surgery	<24 h	Part one: dose escalation; part two: expansion cohort
KSP-910638G (NCT03161418)	HER2	..	Phase 1a	26	..	..	Orally administration of tracer; safety trial in human volunteers
LS301 (NCT02807597)	Integrins	Breast cancer	Phase 1	22	Open surgery	4–24 h	Including evaluation of feasibility for sentinel lymph node detection
LUM015[44]	Cathepsins	Sarcoma and breast cancer	Phase 1	15	Open surgery	2–6 h	Activatable tracer: PEGylated protease-activated
LUM015[45]	Cathepsins	Breast cancer	Phase 2	15	Open surgery	2–6 h	Activatable tracer: PEGylated protease-activated
LUM015 (NCT03321929)	Cathepsins	Breast cancer	Phase 2	250	Open surgery	2–6 h	Activatable tracer: PEGylated protease-activated
LUM015 (NCT03686215)	Cathepsins	Breast cancer	Phase 3	250	Open surgery	2–6 h	Activatable tracer: PEGylated protease-activated
LUM015 (NCT02584244)	Cathepsins	Colorectal, pancreatic, and esophageal cancers	Phase 1/2	21	Open surgery	2–6 h	Activatable tracer: PEGylated protease-activated; fluorescence imaging will only be conducted ex-vivo on resected specimens
LUM015 (NCT03834272)	Cathepsins	Peritoneal metastases	Phase 1	18	Open surgery	2–6 h	Activatable tracer: PEGylated protease-activated
LUM015 (NCT03717142)	Cathepsins	Brain cancer	Phase 1	36	Open surgery	2–6 h	Activatable tracer: PEGylated protease-activated
LUM015 (NCT03441464)	Cathepsins	Prostate cancer	Phase 1	12	Open surgery	2–6 h	Activatable tracer: PEGylated protease-activated; fluorescence imaging will only be conducted ex-vivo on resected specimens
AVB-620[46]	MMPs	Breast cancer	Phase 1	27	Open surgery	2–20 h	Activatable tracer: ratiometric activatable cell-penetrating peptide; part one: dose escalation in 15 patients; part two: expansion cohort of 12 patients
AVB-620 (NCT03113825)	MMPs	Breast cancer	Phase 2	110	Open surgery	<24 h	Activatable tracer: ratiometric activatable cell-penetrating peptide

Some studies share (partially) the same patient population. VATS=video-assisted thoracoscopic surgery. VEGF=vascular endothelial growth factor. EGFR=epidermal growth factor receptor. CEA=carcinoembryonic antigen. CAIX=carbonic anhydrase IX. GRPR=gastrin-releasing peptide receptor. EpCam=epithelial cell adhesion molecule. PSMA=prostate-specific membrane antigen. HER2=human epidermal growth factor receptor 2. MMP=matrix metalloproteinase. HSP=heat shock protein. SPECT= single photon emission computed tomography. PEGylated=attachment of polyethylene glycol.

Table 1: **Ongoing and published clinical trials in molecular fluorescence-guided cancer surgery**

feedback to the surgeon on excised specimens (figure 1). However, detection of lymph node metastases was difficult. Additional studies with bevacizumab-IRDye800CW are planned in endometriosis (NCT02975219), pancreatic cancer (NCT02743975), and perihilar cholangiocarcinoma (NCT03620292).

According to an analogous strategy, the human–mouse chimeric monoclonal antibody cetuximab, which targets the epidermal growth factor receptor (EGFR), was conjugated to IRDye800CW.[29] Rosenthal and colleagues[30] reported no grade 2 or higher adverse events after administration of cetuximab-IRDye800CW in a dose-escalation study with doses up to 62·5 mg/m², which corresponds to 25% of the therapeutic dose of cetuximab, preceded by an injection of 100 mg of unlabelled cetuximab. Furthermore, in-situ mean target-to-background ratio values up to 5·2 were found between head and neck tumours and surrounding tissue. This study[30] also showed the ability of ex-vivo back-table fluorescence imaging to identify positive tumour margins, as well as over resected lesions. Cetuximab-IRDye800CW yielded high sensitivity (97%) and specificity (93%) for the ex-vivo detection of lymph node metastases compared with standard histopathology.[31] This finding suggests that unnecessary neck lymph node dissections could potentially be avoided, eventually resulting in decreased morbidity. A phase 2 clinical trial has been launched in 70 patients with the aim to determine the fluorescent threshold level needed to distinguish tumour tissue from normal tissue (NCT03134846). Tummers and colleagues[33] evaluated the accuracy of the same tracer during pancreatic cancer surgery in seven patients. A sensitivity of 96% and a specificity of 67% were achieved for primary tumour detection, with a mean in-situ target to background ratio value of 2·3. Interestingly, liver metastases were detected by an absence of fluorescence. Tumour positive lymph nodes could also be identified intraoperatively (mean target to background ratio of 6·3). Ex-vivo fluorescence analysis showed a sensitivity of 100% and specificity of 78% macroscopically, and a sensitivity of 91% and specificity of 66% microscopically for detection of metastatic lymph nodes in the optimal dose cohort (50 mg).[34] Cetuximab-IRDye800CW has also been tested in three patients with glioblastoma, of which the two contrast-enhancing tumours on preoperative CT imaging showed fluorescence signal accumulation with a mean ex-vivo target to background ratio of 4·0, whereas the non-contrast-enhancing tumour did not show a clear fluorescence signal (ratio of 1·2).[35]

IRDye800CW-labelled panitumumab, which is a fully humanised monoclonal antibody with improved EGFR binding characteristics compared with cetuximab-IRDye800CW, was clinically evaluated in a dose-escalation study[32] using a loading dose of 100 mg unlabelled panitumumab before surgery to saturate EGFR receptors in normal tissue and therefore optimise tissue contrast. Doses of 0·5 mg/kg and 1 mg/kg allowed in-situ imaging of head and neck tumours with mean target to background ratios between 2·4 and 2·6. Fluorescence imaging was able to detect tumour tissue in the resected specimens with a high sensitivity of 91% and negative predicting value of 93%.[36] Further analysis of the back-table fluorescence imaging data yielded 100% sensitivity for the detection of tumour-positive resection margins (<2 mm), and 95% sensitivity for close resection margins (<5 mm).[37] Furthermore, van Keulen and colleagues[38] showed that fluorescence imaging using panitumumab-IRDye800CW could improve the surgical decision-making in three (21%) of 14 patients with head and neck cancer through the identification of close margins and unanticipated regions of primary disease. In-situ margin assessment has not yet been investigated, although this would be more beneficial for the surgeon to plan and perform the resection during the procedure under fluorescence guidance.

Finally, a 700 nm fluorophore conjugated to SGM-101, an antibody targeting the carcinoembryonic antigen, was evaluated in two pilot studies for 26 patients needing colorectal cancer surgery and 12 patients who needed pancreatic cancer surgery. Tumour-specific fluorescence signals, with the highest target to background ratios (in-vivo 1·8 and ex-vivo 6·1) found in the 10 mg dose group, could be observed with a diagnostic accuracy of 84% in colorectal tumours.[40] In the expansion cohort comprising 17 patients, fluorescence imaging yielded 19 (43%) extra lesions compared with the surgeon's clinical evaluation, resulting in a change of treatment plan in 32% of patients. In patients with pancreatic adenocarcinoma, fluorescence imaging using SGM-101 was able to detect 21 lesions in total, of which one was a false-positive.[39] However, because of the presence of dense desmoplastic stromal tissue surrounding tumour ducts, fluorescence signals and associated target to background ratios were more modest compared with the colorectal cancer group (in-vivo 1·6 and ex-vivo 3·2). Two lesions detected by visual inspection were not fluorescent. The use of SGM-101 could have resulted in a change of treatment plan in one patient, as illustrated in figure 3.

Hybrid fluorescent and radioactive targeted tracers

To overcome the main limitation of near-infrared fluorescence image guidance in terms of the sensitive detection of deeper-lying lesions, use of multimodality imaging has been advocated. Nuclear techniques have been found to be particularly complementary with fluorescence navigation because gamma rays are scarcely attenuated by overlying tissue. In addition to the superficial fluorescent signal, contrast agents featuring both a radioactive label and a fluorescent dye can offer preoperative information for surgical planning via single-photon emission computed tomography or PET imaging

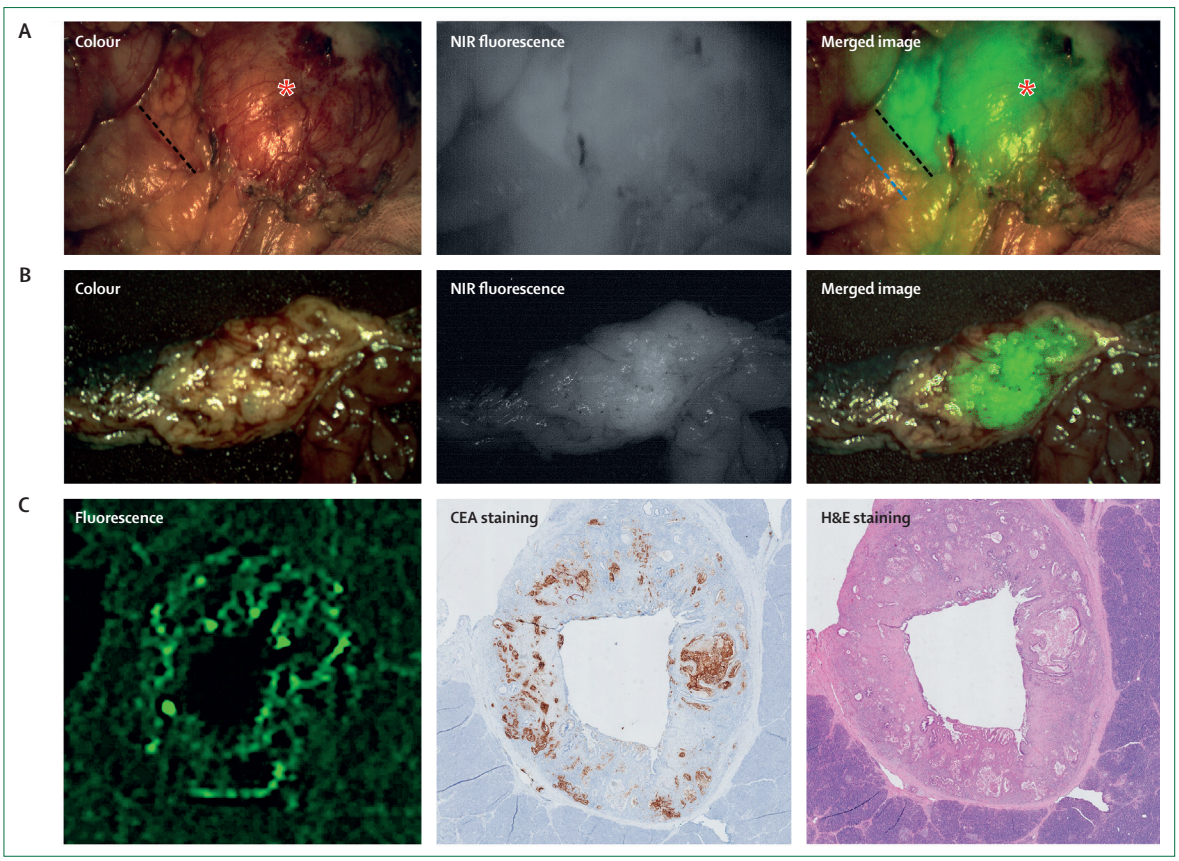

Figure 3: **Example of intraoperative molecular fluorescence imaging during pancreatic surgery**
(A) Intraoperative fluorescence imaging of a pancreatic tumour, which could be visualised using a monoclonal antibody for carcinoembryonic antigen conjugated to a 700 nm fluorophore (SGM-101); however, resection was finally not done due to the presence of peritoneal metastases. On the basis of the image, surgeons decided to move the planned resection line (black dashed line: proposed resection line based on visual inspection and palpation; blue dashed line: proposed resection line based on fluorescence). (B) Ex vivo analysis of a resected pancreatic tumour. (C) Histopathological analysis of a tumour slice of a primary pancreatic tumour showing fluorescence, carcinoembryonic antigen expression, and microscopically localisation of tumour cells. Adapted and reprinted from Hoogstins et al,[39] by permission of Springer Nature. *Tumour bulk.

and acoustic guidance for the surgeon via gamma-probe tracing. ^{99m}Tc-nanocolloid in complex with indocyanine green was the first hybrid tracer tested in humans for refinement of the sentinel lymph node procedure. A prospective trial of 495 patients with head and neck cancer, skin, penile, prostate, or vulva cancer showed the benefit of indocyanine green-^{99m}Tc-nanocolloid in terms of precise visual guidance, depth estimation, and detection of sentinel lymph nodes close to the injection site.[49] However, the intraoperative detection of (lymph node) metastases or occult tumour lesions requires specifically targeted agents.

The monoclonal antibody girentuximab-IRDye800CW co-labelled with ^{111}In was used for the visualisation of clear-cell renal-cell carcinomas, in which carbonic anhydrase IX is overexpressed.[41] Fluorescence imaging was feasible in 12 patients, with high fluorescence in the tumour (mean target to background ratio of 2·5). The added value of the radioguidance consisted in tracing lesions covered with perinephric fat and endophytic lesions. Bombesin, co-labelled with IRDye800CW and ^{68}Ga, was used in 14 patients for detection of glioblastoma multiforma in which the gastrin-releasing peptide receptor is overexpressed. Good correlation between PET signals and intraoperative fluorescence signal was shown. During surgery, most of the tumours showed fluorescence (mean target to background ratio of 4·9), resulting in a sensitivity of 94% and specificity of 100%.[42] With the recent success of radiolabelled prostate-specific membrane antigen (PSMA)-targeted tracers for PET/CT imaging and targeted radionuclide therapy, efforts have also been made towards the design and preclinical validation of hybrid nuclear and fluorescent PSMA-tracers for use as surgical navigation tools in prostate cancer.[50]

Activatable fluorescent agents evaluated in clinical trials

A different strategy to actively trace tumour tissue is by using activatable fluorescent tracers. The fluorescent agent is optically silent until activated, often through enzymatic cleavage of the backbone structure (figure 2).

	Monoclonal antibodies	Antibody fragments		Protein scaffolds	Peptides	Small molecules
		High MW	Low MW			
Size (kDa)	150	80	15–55	3–10	0·5–2·0	0·5–1·0
Delayed scanning time	2–4 days	1–2 days	1–12 h	1–3 h	1–24 h	1–24 h
Tissue penetration	Poor	Medium	Medium/good	Good	Excellent	Excellent
Platform technology	Yes	Yes	Yes	Yes	No	No
Generation strategy	Immunisation	Immunisation	Immunisation	Random mutagenesis; rational design	Rational design	Rational design
Routine production method	Fermentation	Fermentation	Fermentation	Fermentation; chemical synthesis	Chemical synthesis	Chemical synthesis
(cGMP) Production cost	€€€	€€€	€€€	€€€/€	€	€
Subclasses applied in fluorescence-guided surgery	..	Minibody	Fab; diabody; single chain variable fragments; nanobody	Affibody; centyrin; knottin	Linear; cyclic	..

MW=molecular weight. cGMP=current good manufacturing protocols.€€€=very expensive. €=relatively cheaper.

Table 2: **Different classes and subclasses of targeting moieties used for the design of targeted fluorescent contrast agents**

Two activatable fluorescent probes, LUM015 and AVB-620, have been evaluated clinically. Whitley and colleagues[44] described the use of LUM015, which is a cathepsin-activated fluorescent probe, in a phase 1 study in 15 patients with sarcoma or breast cancer. LUM015 was well-tolerated in the three dose groups (0·5 mg/kg, 1·0 mg/kg, and 1·5 mg/kg) and showed tumour-specific fluorescence during ex-vivo imaging with a mean target to background ratio of 4·1 in 13 (87%) patients. Another research group showed the feasibility of LUM015 for intraoperative detection of residual breast cancer in 15 patients.[45] In this cohort, elevated fluorescent signals were noticed in ex-vivo resected breast tumours, resulting in mean target to background ratios of 4·7 in the 0·5 mg/kg group, and 4·2 in the 1·0 mg/kg dose group. Furthermore, for five patients, residual positive margins could be detected in the lumpectomy wall.

Currently, a phase 2 study (NCT03321929) is recruiting patients with breast cancer to determine the efficacy of LUM015 in a larger patient cohort (n=250) and a phase 3 trial (NCT03686215) will start soon afterwards. Next to this, LUM015 is also being evaluated for detection of other cancer types such as gastrointestinal cancers (NCT02584244), peritoneal metastasis (NCT03834272), brain cancer (NCT03717142), or prostate cancer (NCT03441464).

The first clinical use of AVB-620, in breast cancer was described by Unkart and colleagues.This tracer consists of a cell-penetrating peptide bearing a Cy5 fluorophore and a neutralising peptide bearing a Cy7 fluorophore. After proteolytic cleavage, the two peptides are separated, and the Cy5 bearing cell-penetrating peptide will become functional, increasing Cy5 fluorescence intensity and decreasing Cy7 emission. The Cy5/Cy7 fluorescence ratio was used for the analysis of fluorescence signals on resected tumour specimens. 15 patients were included in a dose-escalation cohort and 12 patients in the expansion cohort. Depending on injection time, either 1 day before surgery or on the day of surgery, mean fluorescence ratios of ex-vivo tumour specimens obtained were 1·1 or 1·9 for cancerous breast tissue, and 0·6 or 1·2 for adjacent normal breast tissue. Based on these results a phase 2 trial (NCT03113825) has been launched to determine the accuracy of AVB-620 for distinguishing malignant and nonmalignant breast tissue.

Emerging targeted fluorescent molecular tracers with improved pharmacokinetics and specificity

The inherent capacity of antibodies to effectively recognise specific cell-surface expressed antigens and the relatively easy process through which new antibodies can be generated, makes them the biggest class of readily available targeted agents. Therefore, many groups are currently evaluating preclinically novel near-infrared fluorescence-labelled antibodies targeting alternative biomarkers for distinct intraoperative imaging applications, all showing the feasibility of the antibodies to highlight tumour lesions.[51–54] The long blood retention of antibodies due to their large size and neonatal Fc receptor-mediated recycling, in combination with the enhanced permeability and retention effect, has been associated with long delayed imaging times (several days between the moment of injection and the surgery) and non-specific tissue accumulation resulting in false-positive signals.[33,40,55] Furthermore, antibodies are known to show poor tissue penetration at microscopic level (table 2).[56]

Advances in protein engineering have led to the development of antibody fragments (minibodies, Fab-fragments, diabodies,[57] and single chain variable fragments) (figure 2, table 2) that retain similar binding characteristics, but show better tumour penetration and more rapid clearance from non-targeted tissues. For example, Zhang and colleagues[58] showed that the IRDye800CW-labelled minibody that is specific to the prostate stem-cell antigen facilitated complete resection of invasive tumours and detection of tumour-infiltrated lymph nodes in mice. A clinical trial with the minibody

IAB2M-IRDye800CW that is specific to prostate specific membrane antigen has been launched with the aim of evaluating the safety, feasibility, and optimal dose of the contrast agent to visualise cancer invasion in 20 patients. In a second stage, the effect of fluorescence imaging guidance on the completeness of tumour resection, urinary and sexual function outcome, disease recurrence, and survival will also be assessed in 50 men who are scheduled for robot-assisted laparoscopic radical prostatectomy (ISRCTN10046036).

Antibody-fragments with a low molecular weight (<60 kDa in size) that are rapidly eliminated from the blood via renal excretion have especially been researched as tools for molecular imaging applications because they enable highly specific and high-contrast imaging at early timepoints after injection.[59] However, the conjugation of near-infrared fluorescent dyes (such as IRDye800CW) can cause increased albumin binding and hepatic clearance of the tracers, and that can possibly influence their typical pharmacokinetic profile.[60] The Fab-fragment VB6–845-IRDye800CW, which targets the epithelial cell adhesion molecule highly overexpressed on most epithelial cancers, showed high target to background ratios between 8 and 24 h after injection in orthotopic breast and colorectal tumour mouse models.[61] This tracer has been produced for clinical use and a phase 1 trial (NL7363) is planned in patients with oesophageal, gastric, or rectosigmoid cancer who will have laparoscopic surgery. Researchers have also been interested in single-domain antibodies, better known as nanobodies™, which are derived from heavy-chain antibodies found in camelids. Several fluorescently-labelled nanobodies, targeting tumour markers such as carbonic anhydrase IX or HER2 have been successfully evaluated in preclinical models, with noteworthy tumour to background ratios reached within 1 to 3 h after injection.[62,63]

Another class of targeted agents that have elicited interest are non-immunoglobulin protein scaffolds, which include centyrins, affibodies, or cystine knottins (figure 2).[64–66] These scaffolds exhibit similar pharmacokinetics as the small antibody fragments, but are generated through random mutagenesis or rational design of the antigen-binding regions, instead of via immunisation in which the affinity of molecules for their antigen is matured naturally in an animal. For example, the IRDye800CW-labelled anti-EGFR affibody molecule ABY-029 showed high-uptake and high-contrast values on ex-vivo slices compared with normal brain tissue in an intracranial glioma rat model within 1 h after injection.[67] ABY-029 is under investigation in three phase 1 clinical trials; one for recurrent glioma (NCT02901925), another for primary sarcoma (NCT03154411), and one in head and neck cancer surgery (NCT03282461). In addition to the clinically tested tozuleristide, Tummers and colleagues[65] validated another cystine knottin peptide binding specifically to integrin $\alpha_v\beta_6$ in orthotopic and spontaneous transgenic pancreatic tumour models.

Peptides and small molecules are even smaller in size than the compounds above; however, the pharmacokinetic profile of each tracer becomes dependent on their individual physicochemical characteristics. In comparison with platform technologies such as antibodies, antibody fragments, and protein scaffolds high throughput generation of novel peptides and small molecules with adequate properties for in-vivo imaging is more difficult and unpredictable. However, once a lead compound against a specific biomarker has been identified, it can be routinely produced according to current good manufacturing protocols for clinical use at a much lower cost than biologicals, which require production through fermentation (table 2). Bombesin-antagonists[68] and RGD peptides[69] are often subject to preclinical investigation. Besides IRdye800CW and Cy5, cRGD has also been conjugated with zwitterionic fluorophore ZW800–1. cRGD-ZW800–1 exhibits substantially less non-specific binding in normal organs and tissues than does IRDye800CW-labelled cRGD, and is cleared exclusively through the kidneys.[70] A drawback of ZW800–1 is its instability over time in serum, although it appears that this limitation can be overcome by rapid internalisation.[71] Using cRGD-ZW800–1, Handgraaf and colleagues[69] showed the feasibility to image integrin overexpression on malignant and neoangiogenic cells in various tumour models, including pancreas, colorectal, oral, and breast cancer with high tumour signals and tumour to background ratios at 4 h after injection. Moreover, tumour signals were still clearly distinguishable after 24 and even after 48 h. Because of the easy production procedure and low cost, this probe is undergoing clinical translation and the first human data are expected in the near future (NL7724; table 1).

Challenges and considerations towards clinical translations of novel tracers

A wide variety of molecular tracers have shown potential to specifically highlight tumour lesions in animal models and are awaiting clinical translation. The field of PET imaging, which is considerably more advanced regarding the development of targeted tracers, favours the use of highly specific agents with fast pharmacokinetics, both from a safety and practical point of view. Analogously, for fluorescence imaging applications, the timing of administration of the contrast agent (eg, just before surgery would be highly convenient) and the clearing pattern of the agent need to be considered. For example, renally cleared agents would permit improved visualisation of liver lesions in comparison with fluorescent agents cleared via the hepatobiliary route.[59] However, because the minimal signal level that must be reached for sensitive detection with fluorescence imaging devices is higher than for PET, slower blood clearance rates could enhance signal intensities at the target. Dose optimisation studies are therefore essential to obtain superior image quality in terms of both signal intensity

and tumour to background ratios. Yet, the use of highly sensitive imaging instruments and the design of brighter fluorescent dyes are probably more advisable approaches towards clinical translation than increasing the injected dose of rapidly cleared targeted contrast agents to improve detection's sensitivity because of potential toxicity.

Despite all preclinical evidence, the real assessment of the value of fluorescent contrast agents for intra-operative imaging can only be performed in humans. Hereto, promising compounds have to undergo a translational process before clinical trials can be initiated. Current good manufacturing practice and toxicity studies remain the main bottlenecks of development because of their cost and time-consuming administrative burden. Because targeted fluorescent contrast agents often require doses above the microdosing level, a simplified regulation with less extensive toxicity studies as for radiopharmaceuticals is unfortunately not possible. Fast clearing tracers with predictable biodistributions could eventually have an advantage regarding documentation of the intended use because they are less likely to elicit unpredictable toxicity issues. Furthermore, the choice for a targeting moiety will have to be balanced between the ease of generation (derived from a generic platform technology) and the cost for routine production (relatively cheap chemical synthesis *vs* expensive fermentation process). For the field of intraoperative fluorescence imaging, this is even more important because the financial added value is probably less than for cancer therapeutics or companion diagnostic PET tracers.

The effectiveness of a molecular tracer will not only be determined by its general pharmacokinetic profile but will also be highly dependent on the biomarker it is intended to recognise and its expression pattern. Unfortunately, so far, no clear consensus exists on the most optimal biomarkers for the field. Yet, many prerequisites have been defined; these include: the biomarker should be highly overexpressed on tumour cells or stroma, while presenting no or low expression on normal tissue or after chemotherapy or radiotherapy to ensure high-contrast and specific imaging of only the tissue of interest; biomarkers are preferred to be extracellularly expressed to permit targeting by molecules that do not penetrate cells, but should ideally also internalise after binding for a long-lasting signal; the biomarker should show specificity across at least different types and subtypes of cancers to avoid preoperative screening of patients (unlike nuclear medicine applications for which lately targeting of highly specific biomarkers is most often warranted to enable patient stratification for personalised therapies); and within one tumour type, homogeneous expression throughout the cancerous tissue is warranted, independently of tumour stage. However, most human tumours are known to exhibit substantial spatial and temporal intratumour heterogeneity, and this aspect is particularly difficult to mimic in preclinical models. Therefore, in-vivo efficacy shown in preclinical research can often not be directly extrapolated to the clinical setting. From a regulatory and economic point of view, the feasibility of administrating a cocktail of fluorescent molecular tracers to overcome tumour heterogeneity has been suggested but is unlikely.

Future perspectives

Intraoperative fluorescence molecular imaging is still in its infancy. Clinical studies completed so far mainly consist of early-phase trials aimed at evaluating the safety of fluorescent contrast agents, estimating the optimal dose, showing feasibility of intraoperative lesion detection, and assessing exploratory data on sensitivity and specificity. It has been shown that near-infrared fluorescence imaging can improve the detection of peritoneal lesions during cytoreductive surgery, which is associated with improved survival. However, the primary solid tumour types for which surgical margin assessment and intraoperative staging (ie, detection of lymph node or distant metastases) would be most beneficial, is not yet established. On the one hand, depending on the desired distance of the resection margin, in-situ molecular fluorescence imaging could be supportive to plan surgical dissection planes or to visualise remnant tumour cells after resection. On the other hand, surgical specimen imaging could be complementary and could provide precise information about both the extent of the tumour and the resection margins. When close resection margins are encountered, an additional resection could be considered and performed.

Large, multicentre, randomised controlled trials are thus mandatory to find out the diagnostic accuracy of fluorescence molecular imaging and to show the value of this technique on surgical outcomes and benefits to the patient. To convince regulatory authorities and reimbursement agencies, it is essential to identify clinically meaningful endpoints and surrogates of clinical benefit that are acceptable to authorities. A phase 3 multicentre, randomised controlled trial (NCT03659448) has been launched in patients with metastastic colorectal cancer to prove the added value of imaging with SGM-101 targeting anti-carcinoembryonic antigen in terms of resection margins. Furthermore, a phase 3 trial (NCT03180307) with OTL-38 is underway and includes patients with ovarian cancer who are scheduled to have open debulking surgery. In this study, the efficacy, which has been defined as the proportion of patients in which fluorescence imaging yields at least one additional tumour-positive lesion compared with normal conditions, will be assessed, as well as the diagnostic accuracy of OTL-38 at the patient level.

Nevertheless, the absence of a general consensus on standardised protocols for the clinical evaluation of new molecular fluorescent agents makes the conduction of multicentre trials and the comparison between clinical studies difficult. For example, tumour to background ratio is an important determinant for evaluating the efficacy of

Search strategy and selection criteria

References for this Review were identified by searching PubMed using the search terms "fluorescence", "near-infrared fluorescence", "optical imaging", "image guided surgery", "fluorescence guided surgery", "molecular imaging", "hybrid imaging", "fluorescent tracer", "targeted fluorescent tracers", "activatable tracers" and "IRDye800CW". References published on or before Feb 28, 2019 were considered. Articles were also identified through searches of the authors' own files. Only papers published in the English language were reviewed. The final reference list was generated on the basis of originality and relevance to the broad scope of this Review. Additionally, ClinicalTrials.gov, Dutch Trial Register, and ISRCTN registry were searched for ongoing and registered clinical trials using the same terms as mentioned above.

a fluorescent tracer; however, calculating tumour to background ratios could be influenced by selection bias of relevant regions of interest, and studies report tumour to background ratios measured in different circumstances (eg, in-vivo or ex-vivo). Furthermore, detected signal intensities not only depend on the chemical, photochemical, and biological characteristics of the fluorescent agent being investigated; but are also affected by tissue optical factors, depth of signal, as well as by the technical specifications and performance of the chosen imaging instrument. Importantly, the fluorescence imaging system should match the fluorescent contrast agent for optimal detection. Despite considerable efforts towards the development of a universal tool for calibration, quality control, and benchmarking of imaging devices, its development remains challenging because of the diversity of parameters influencing imaging.[72] Alternatively, advances in methods and models supporting accurate quantification of fluorophore concentrations in tissue would enable more objective distinction between tumour or non-tumour tissue. Improved image processing and interpretation would be desirable for the determination of clinically relevant cut off values for resection margins and exclusion of false-positive signals.[73] Meanwhile, guidelines regarding experimental workflow, data collection, image analysis, and reporting have emerged.[74–76] These are intended to obtain reliable, reproducible, and comparable data that will eventually ensure clinical implementation and approval of the technique.

Besides adequate open-surgery fluorescent imaging devices currently available, many laparoscopic and robotic surgical systems are already equipped with fluorescence cameras. It is to be expected that, in the future, more and more complex surgeries will be performed in a minimally invasive way, because they have already shown substantial benefits and led to a reduction in hospital costs.[77] With minimally invasive surgeries, it is even more important to guide the surgeon because of the limited field of view, associated risk of missing hidden lesions, and the absence of tactile feedback. However, it is also important to simultaneously highlight vital structures such as ureters or nerves, in addition to tumour tissue. During such procedures, the combination of fluorophores would be beneficial (eg, one for tumour detection and one for detection of other important structures or tissue perfusion). This can be achieved by using fluorescence camera systems that are equipped with two or more fluorescent channels.

Conclusion

Fluorescence molecular imaging has so far shown its potential to support surgical procedures and the feasibility to improve clinical outcomes. Although there is much enthusiasm about these first results, intraoperative fluorescence molecular imaging is now at a crucial turning point in which unequivocal efficacy studies are needed to move the field beyond current proof of concept studies to produce a real change in clinical practice. Once this step has been taken, more extensive investments are to be expected towards novel tracers with improved characteristics pertaining to pharmacokinetics and specificity, as well as more sophisticated image analysis software. An important asset of fluorescence imaging is the relative ease by which the technology can be integrated within the routine of many different surgical and interventional cases, hence the necessity for centres of expertise to train users, as well as to create wide-spread awareness of the technique.

Contributors

SH and LvM contributed to the conception and writing of the Review. SH, LvM, and PD were involved in the literature search and conceptualisation of the figures. All authors critically revised and approved the manuscript for publication.

Declaration of interests

We declare no competing interests.

Acknowledgments

SH and PD are supported by the Belgian Foundation Against Cancer and the IOF-Gear programme. LvM received funding by the European Union Horizon 2020 programme (grant 692470). JSDM is supported by the Bas Mulder Award (grant UL2015–7665) from the Alpe d'HuZes foundation/Dutch Cancer Society. ALV received funding from the Dutch Cancer Society (grant UL2015–8089 and UL2018–11363).

References

1 Tilly C, Lefevre JH, Svrcek M, et al. R1 rectal resection: look up and don't look down. *Ann Surg* 2014; **260:** 794–49.

2 Wong LS, McMahon J, Devine J, et al. Influence of close resection margins on local recurrence and disease-specific survival in oral and oropharyngeal carcinoma. *Br J Oral Maxillofac Surg* 2012; **50:** 102–08.

3 Esposito I, Kleeff J, Bergmann F, et al. Most pancreatic cancer resections are R1 resections. *Ann Surg Oncol* 2008; **15:** 1651–60.

4 Vos EL, Gaal J, Verhoef C, Brouwer K, van Deurzen CHM, Koppert LB. Focally positive margins in breast conserving surgery: predictors, residual disease, and local recurrence. *Eur J Surg Oncol* 2017; **43:** 1846–54.

5 Stammes MA, Bugby SL, Porta T, et al. Modalities for image- and molecular-guided cancer surgery. *Br J Surg* 2018; **105:** e69–83.

6 Gioux S, Choi HS, Frangioni JV. Image-guided surgery using invisible near-infrared light: fundamentals of clinical translation. *Mol Imaging* 2010; **9:** 237–55.

7 van Manen L, Handgraaf HJM, Diana M, et al. A practical guide for the use of indocyanine green and methylene blue in fluorescence-guided abdominal surgery. *J Surg Oncol* 2018; **118:** 283–300.

8 Stummer W, Pichlmeier U, Meinel T, et al. Fluorescence-guided surgery with 5-aminolevulinic acid for resection of malignant glioma: a randomised controlled multicentre phase III trial. *Lancet Oncol* 2006; **7:** 392–401.

9 Grossman HB, Stenzl A, Fradet Y, et al. Long-term decrease in bladder cancer recurrence with hexaminolevulinate enabled fluorescence cystoscopy. *J Urol* 2012; **188:** 58–62.

10 Hadjipanayis CG, Widhalm G, Stummer W. What is the surgical benefit of utilizing 5-aminolevulinic acid for fluorescence-guided surgery of malignant gliomas? *Neurosurgery* 2015; **77:** 663–73.

11 Vahrmeijer AL, Hutteman M, van der Vorst JR, van de Velde CJ, Frangioni JV. Image-guided cancer surgery using near-infrared fluorescence. *Nat Rev Clin Oncol* 2013; **10:** 507–18.

12 van Dam GM, Themelis G, Crane LM, et al. Intraoperative tumor-specific fluorescence imaging in ovarian cancer by folate receptor-alpha targeting: first in-human results. *Nat Med* 2011; **17:** 1315–19.

13 Kennedy GT, Okusanya OT, Keating JJ, et al. The optical biopsy: a novel technique for rapid intraoperative diagnosis of primary pulmonary adenocarcinomas. *Ann Surg* 2015; **262:** 602–09.

14 Okusanya OT, DeJesus EM, Jiang JX, et al. Intraoperative molecular imaging can identify lung adenocarcinomas during pulmonary resection. *J Thorac Cardiovasc Surg* 2015; **150:** 28–35.

15 Tummers QR, Hoogstins CE, Gaarenstroom KN, et al. Intraoperative imaging of folate receptor alpha positive ovarian and breast cancer using the tumor specific agent EC17. *Oncotarget* 2016; **7:** 32144–55.

16 Guzzo TJ, Jiang J, Keating J, et al. Intraoperative molecular diagnostic imaging can identify renal cell carcinoma. *J Urol* 2016; **195:** 748–55.

17 Hoogstins CE, Tummers QR, Gaarenstroom KN, et al. A novel tumor-specific agent for intraoperative near-infrared fluorescence imaging: a translational study in healthy volunteers and patients with ovarian cancer. *Clin Cancer Res* 2016; **22:** 2929–38.

18 Shum CF, Bahler CD, Low PS, et al. Novel use of folate-targeted intraoperative fluorescence, OTL38, in robot-assisted laparoscopic partial nephrectomy: report of the first three cases. *J Endourol Case Rep* 2016; **2:** 189–97.

19 Predina JD, Newton AD, Keating J, et al. Intraoperative molecular imaging combined with positron emission tomography improves surgical management of peripheral malignant pulmonary nodules. *Ann Surg* 2017; **266:** 479–88.

20 Predina JD, Newton A, Connolly C, Singhal S. Folate receptor-targeted molecular imaging improves identification of malignancy during pulmonary resection: a case report. *J Cardiothorac Surg* 2017; **12:** 110.

21 Predina JD, Newton AD, Xia L, et al. An open label trial of folate receptor-targeted intraoperative molecular imaging to localize pulmonary squamous cell carcinomas. *Oncotarget* 2018; **9:** 13517–29.

22 Predina JD, Newton AD, Keating J, et al. A phase I clinical trial of targeted intraoperative molecular imaging for pulmonary adenocarcinomas. *Ann Thorac Surg* 2018; **105:** 901–08.

23 Predina JD, Newton AD, Connolly C, et al. Identification of a folate receptor-targeted near-infrared molecular contrast agent to localize pulmonary adenocarcinomas. *Mol Ther* 2018; **26:** 390–403.

24 Predina JD, Newton A, Corbett C, et al. Localization of pulmonary ground-glass opacities with folate receptor-targeted intraoperative molecular imaging. *J Thorac Oncol* 2018; **13:** 1028–36.

25 Pierce JT, Cho SS, Nag S, et al. Folate receptor overexpression in human and canine meningiomas-immunohistochemistry and case report of intraoperative molecular imaging. *Neurosurgery*; published online Aug 3, 2018. DOI: 10.1093/neuros/nyy356.

26 Boogerd LSF, Hoogstins CES, Gaarenstroom KN, et al. Folate receptor-alpha targeted near-infrared fluorescence imaging in high-risk endometrial cancer patients: a tissue microarray and clinical feasibility study. *Oncotarget* 2018; **9:** 791–801.

27 Harlaar NJ, Koller M, de Jongh SJ, et al. Molecular fluorescence-guided surgery of peritoneal carcinomatosis of colorectal origin: a single-centre feasibility study. *Lancet Gastroenterol Hepatol* 2016; **1:** 283–90.

28 Lamberts LE, Koch M, de Jong JS, et al. Tumor-specific uptake of fluorescent bevacizumab-IRDye800CW microdosing in patients with primary breast cancer: a phase I feasibility study. *Clin Cancer Res* 2017; **23:** 2730–41.

29 de Boer E, Warram JM, Tucker MD, et al. In vivo fluorescence immunohistochemistry: localization of fluorescently labeled cetuximab in squamous cell carcinomas. *Sci Rep* 2015; **5:** 10169.

30 Rosenthal EL, Warram JM, de Boer E, et al. Safety and tumor specificity of cetuximab-IRDye800 for surgical navigation in head and neck cancer. *Clin Cancer Res* 2015; **21:** 3658–66.

31 Rosenthal EL, Moore LS, Tipirneni K, et al. Sensitivity and specificity of cetuximab-IRDye800CW to identify regional metastatic disease in head and neck cancer. *Clin Cancer Res* 2017; **23:** 4744–52.

32 Gao RW, Teraphongphom N, de Boer E, et al. Safety of panitumumab-IRDye800CW and cetuximab-IRDye800CW for fluorescence-guided surgical navigation in head and neck cancers. *Theranostics* 2018; **8:** 2488–95.

33 Tummers WS, Miller SE, Teraphongphom NT, et al. Intraoperative pancreatic cancer detection using tumor-specific multimodality molecular imaging. *Ann Surg Oncol* 2018; **25:** 1880–88.

34 Tummers WS, Miller SE, Teraphongphom NT, et al. Detection of visually occult metastatic lymph nodes using molecularly targeted fluorescent imaging during surgical resection of pancreatic cancer. *HPB (Oxford)* 2019; published online Feb 2. DOI:10.1016/j.hpb.2018.11.008.

35 Miller SE, Tummers WS, Teraphongphom N, et al. First-in-human intraoperative near-infrared fluorescence imaging of glioblastoma using cetuximab-IRDye800. *J Neurooncol* 2018; **139:** 135–43.

36 Gao RW, Teraphongphom NT, van den Berg NS, et al. Determination of tumor margins with surgical specimen mapping using near-infrared fluorescence. *Cancer Res* 2018; **78:** 5144–54.

37 van Keulen S, van den Berg NS, Nishio N, et al. Rapid, non-invasive fluorescence margin assessment: optical specimen mapping in oral squamous cell carcinoma. *Oral Oncol* 2019; **88:** 58–65.

38 van Keulen S, Nishio N, Fakurnejad S, et al. The clinical application of fluorescence-guided surgery in head and neck cancer. *J Nucl Med* 2019; published online Feb 7. DOI:10.2967/jnumed.118.222810.

39 Hoogstins CES, Boogerd LSF, Sibinga Mulder BG, et al. Image-guided surgery in patients with pancreatic cancer: first results of a clinical trial using SGM-101, a novel carcinoembryonic antigen-targeting, near-infrared fluorescent agent. *Ann Surg Oncol* 2018; **25:** 3350–57.

40 Boogerd LSF, Hoogstins CES, Schaap DP, et al. Safety and effectiveness of SGM-101, a fluorescent antibody targeting carcinoembryonic antigen, for intraoperative detection of colorectal cancer: a dose-escalation pilot study. *Lancet Gastroenterol Hepatol* 2018; **3:** 181–91.

41 Hekman MC, Rijpkema M, Muselaers CH, et al. tumor-targeted dual-modality imaging to improve intraoperative visualization of clear cell renal cell carcinoma: a first in man study. *Theranostics* 2018; **8:** 2161–70.

42 Li D, Zhang J, Chi C, et al. First-in-human study of PET and optical dual-modality image-guided surgery in glioblastoma using (68)Ga-IRDye800CW-BBN. *Theranostics* 2018; **8:** 2508–20.

43 Dintzis SM, Hansen S, Harrington KM, et al. Real-time visualization of breast carcinoma in pathology specimens from patients receiving fluorescent tumor-marking agent tozuleristide. *Arch Pathol Lab Med*; published online Dec 14, 2018. DOI:10.5858/arpa.2018-0197-OA.

44 Whitley MJ, Cardona DM, Lazarides AL, et al. A mouse-human phase 1 co-clinical trial of a protease-activated fluorescent probe for imaging cancer. *Sci Transl Med* 2016; **8:** 320ra4.

45 Smith BL, Gadd MA, Lanahan CR, et al. Real-time, intraoperative detection of residual breast cancer in lumpectomy cavity walls using a novel cathepsin-activated fluorescent imaging system. *Breast Cancer Res Treat* 2018; **171:** 413–20.

46 Unkart JT, Chen SL, Wapnir IL, Gonzalez JE, Harootunian A, Wallace AM. Intraoperative tumor detection using a ratiometric activatable fluorescent peptide: a first-in-human phase 1 study. *Ann Surg Oncol* 2017; **24:** 3167–73.

47 van Leeuwen FW, Valdés-Olmos R, Buckle T, Vidal-Sicart S. Hybrid surgical guidance based on the integration of radionuclear and optical technologies. *Br J Radiol* 2016; **89:** 20150797.

48 Brouwer OR, Buckle T, Vermeeren L, et al. Comparing the hybrid fluorescent-radioactive tracer indocyanine green-99mTc-nanocolloid with 99mTc-nanocolloid for sentinel node identification: a validation study using lymphoscintigraphy and SPECT/CT. *J Nucl Med* 2012; **53:** 1034–40.

49 KleinJan GH, van Werkhoven E, van den Berg NS, et al. The best of both worlds: a hybrid approach for optimal pre- and intraoperative identification of sentinel lymph nodes. *Eur J Nucl Med Mol Imaging* 2018; **45:** 1915–25.

50 Schottelius M, Wurzer A, Wissmiller K, et al. Synthesis and preclinical characterization of the PSMA-targeted hybrid tracer PSMA-I&F for nuclear and fluorescence imaging of prostate cancer. *J Nucl Med* 2019; **60:** 71–78.

51 Odenthal J, Rijpkema M, Bos D, et al. Targeting CD44v6 for fluorescence-guided surgery in head and neck squamous cell carcinoma. *Sci Rep* 2018; **8:** 10467.

52 Boonstra MC, Van Driel PB, Keereweer S, et al. Preclinical uPAR-targeted multimodal imaging of locoregional oral cancer. *Oral Oncol* 2017; **66:** 01–08.

53 Lwin TM, Miyake K, Murakami T, et al. Fluorescent humanized anti-CEA antibody specifically labels metastatic pancreatic cancer in a patient-derived orthotopic xenograft (PDOX) mouse model. *Oncotarget* 2018; **9:** 37333–42.

54 van Driel PB, Boonstra MC, Prevoo HA, et al. EpCAM as multi-tumour target for near-infrared fluorescence guided surgery. *BMC Cancer* 2016; **16:** 884.

55 Warram JM, de Boer E, Moore LS, et al. A ratiometric threshold for determining presence of cancer during fluorescence-guided surgery. *J Surg Oncol* 2015; **112:** 02–08.

56 Xenataki KT, Oliveira S, van Bergen en Henegouwen PM. Antibody or antibody fragments-implications for molecular imaging and targeted therapy of solid tumors. *Front Immunol* 2017; **8:** 1287.

57 Sonn GA, Behesnilian AS, Jiang ZK, et al. Fluorescent image-guided surgery with an anti-prostate stem cell antigen (PSCA) diabody enables targeted resection of mouse prostate cancer xenografts in real time. *Clin Cancer Res* 2016; **22:** 1403–12.

58 Zhang M, Kobayashi N, Zettlitz KA, et al. Near-infrared dye-labeled anti-prostate stem cell antigen minibody enables real-time fluorescence imaging and targeted surgery in translational mouse models. *Clin Can Res* 2019; **25:** 188–200.

59 Krasniqi A, D'Huyvetter M, Devoogdt N, et al. Same-day imaging using small proteins: clinical experience and translational prospects in oncology. *J Nucl Med* 2018; **59:** 885–91.

60 Debie P, Van Quathem J, Hansen I, et al. Effect of dye and conjugation chemistry on the biodistribution profile of near-infrared-labeled nanobodies as tracers for image-guided surgery. *Mol Pharm* 2017; **14:** 1145–53.

61 Boogerd LSF, Boonstra MC, Prevoo HAJM, et al. Fluorescence-guided tumor detection with a novel anti-EpCAM targeted antibody fragment: preclinical validation. *Surg Oncol* 2019; **28:** 01–08.

62 Debie P, Vanhoeij M, Poortmans N, et al. Improved debulking of peritoneal tumor implants by near-infrared fluorescent nanobody image guidance in an experimental mouse model. *Mol Imaging Biol* 2018; **20:** 361–67.

63 van Brussel AS, Adams A, Oliveira S, et al. Hypoxia-targeting fluorescent nanobodies for optical molecular imaging of pre-invasive breast cancer. *Mol Imaging Biol* 2016; **18:** 535–44.

64 Mahalingam SM, Dudkin VY, Goldberg S, et al. Evaluation of a centyrin-based near-infrared probe for fluorescence-guided surgery of epidermal growth factor receptor positive tumors. *Bioconjug Chem* 2017; **28:** 2865–73.

65 Tummers WS, Kimura RH, Abou-Elkacem L, et al. Development and preclinical validation of a cysteine knottin peptide targeting integrin alphavbeta6 for near-infrared fluorescent-guided surgery in pancreatic cancer. *Clin Cancer Res* 2018; **24:** 1667–76.

66 Samkoe KS, Gunn JR, Marra K, et al. Toxicity and pharmacokinetic profile for single-dose injection of ABY-029: a fluorescent anti-EGFR synthetic affibody molecule for human use. *Mol Imaging Biol* 2017; **19:** 512–21.

67 de Souza AL, Marra K, Gunn J, et al. Fluorescent affibody molecule administered in vivo at a microdose level labels EGFR expressing glioma tumor regions. *Mol Imaging Biol* 2017; **19:** 41–48.

68 Xu H, Bandari RP, Lee L, et al. Design, synthesis, and in vitro and in vivo evaluation of high affinity and specificity near-infrared fluorescent bombesin antagonists for tumor imaging. *J Med Chem* 2018; **61:** 7657–70.

69 Handgraaf HJM, Boonstra MC, Prevoo H, et al. Real-time near-infrared fluorescence imaging using cRGD-ZW800–1 for intraoperative visualization of multiple cancer types. *Oncotarget* 2017; **8:** 21054–66.

70 Choi HS, Gibbs SL, Lee JH, et al. Targeted zwitterionic near-infrared fluorophores for improved optical imaging. *Nat Biotechnol* 2013; **31:** 148–53.

71 Hyun H, Owens EA, Narayana L, et al. Central C-C bonding increases optical and chemical stability of NIR fluorophores. *RSC Adv* 2014; **4:** 58762–68.

72 Koch M, Symvoulidis P, Ntziachristos V. Tackling standardization in fluorescence molecular imaging. *Nature Photonics* 2018; **12:** 505–15.

73 Valdes PA, Angelo JP, Choi HS, Gioux S. qF-SSOP: real-time optical property corrected fluorescence imaging. *Biomed Opt Express* 2017; **8:** 3597–605.

74 Koller M, Qiu SQ, Linssen MD, et al. Implementation and benchmarking of a novel analytical framework to clinically evaluate tumor-specific fluorescent tracers. *Nat Commun* 2018; **9:** 3739.

75 Tummers WS, Warram JM, van den Berg NS, et al. Recommendations for reporting on emerging optical imaging agents to promote clinical approval. *Theranostics* 2018; **8:** 5336–47.

76 Pogue BW, Zhu TC, Ntziachristos V, et al. Fluorescence-guided surgery and intervention—an AAPM emerging technology blue paper. *Med Phys* 2018; **45:** 2681–88.

77 Braga M, Vignali A, Zuliani W, Frasson M, Di Serio C, Di Carlo V. Laparoscopic versus open colorectal surgery: cost-benefit analysis in a single-center randomized trial. *Ann Surg* 2005; **242:** 890–95.